scientific reports

Check for updates

OPEN

Unraveling the metabolic activities of bioactive compounds on cellular models of hepatosteatosis and adipogenesis through docking analysis with PPARs

Farah Diab[1,3], Hawraa Zbeeb[1], Lama Zeaiter[1,2], Francesca Baldini[2], Aldo Pagano[3], Velia Minicozzi[4] & Laura Vergani[1]✉

Obesity is associated with fatty liver disease. Available therapies show modest efficacy, and nutraceuticals with good effectiveness and safety are largely investigated. We focused on five natural compounds, three plant phenolic compounds (carvacrol, rosmarinic acid, silybin), and two thyroid hormones (T2: 3,5-diiodo-l-thyronine; T3: 3,5,3′-triiodo-L-thyronine) as comparison, to assess their beneficial effects on two cellular models of hepatosteatosis and adipogenesis. All compounds ameliorated the lipid accumulation and oxidative stress in both models, but with different potencies. The peroxisome proliferator-activated receptors (PPARs) are pivotal controllers of adipogenesis and lipid metabolism. For the main isoforms, PPARγ and PPARa, we assessed their possible binding to the compounds by molecular docking calculations, and their expression pattern by real-time PCR. All compounds bind both PPARs with different affinity, while not all compounds affect their expression. The results may clarify the distinctive molecular mechanisms underlying the action of the five compounds in the different cell models with possible applications to treat obesity.

Keywords Natural products, Hepatosteatosis, Adipogenesis, Metabolic activities, Nuclear receptors, Molecular Docking

Abbreviations

T2	3,5-Diiodo-l-thyronine
T3	3,5,3'-Triiodo-L-thyronine
CVL	Carvacrol
DBD	DNA-binding domain
FAs	Fatty acids
LBD	Ligand-binding domain
MDA	Malondialdehyde
MS	Metabolic syndrome
3T3-L1	Mouse pre-adipocyte cell-line
NAFLD	Nonalcoholic fatty liver disease
PPARs	Peroxisome proliferator-activated receptors
PPARα	Peroxisome proliferator-activated receptors alpha
PPARγ	Peroxisome proliferator-activated receptors gamma
PC	Phenolic compounds
FaO	Rat hepatoma cell-line
ROS	Reactive oxygen species
RA	Rosmarinic acid
SIL	Silybin

[1]DISTAV, Department for the Earth, Environment and Life Sciences, University of Genova, Corso Europa 26, 16132 Genova, Italy. [2]Istituto Italiano Tecnologia, Genova, Italy. [3]DIMES, Department of Experimental Medicine, University of Genoa, Genova, Italy. [4]Department of Physics, University of Rome Tor Vergata and INFN - Section of Rome Tor Vergata, Rome, Italy. ✉email: laura.vergani@unige.it

TG	Triglyceride
ΔG	Binding energy
Ki	Inhibition constant

Metabolic syndrome (MS) is a clinical condition characterized by a cluster of abnormalities, including visceral obesity, fatty liver, dyslipidemia, hyperinsulinemia, insulin resistance, and type 2 diabetes mellitus (T2DM)[1]. Obesity is a complex disorder defined by visceral fat depot due to excess caloric intake and physical inactivity in genetically susceptible individuals; in Caucasian population obesity is diagnosed by a body mass index (BMI) $\geq 30 kg/m^2$. In parallel with the escalating prevalence of obesity worldwide, the nonalcoholic fatty liver disease (NAFLD) is also increasing[2]. In fact, a mechanistic interplay connects NAFLD with adipose tissue hypertrophy and obesity[3]. Although many drugs have been proposed to treat obesity and NAFLD, their side effects make them poorly attractive, and the current recommended alternative relies on lifestyle modifications, including diet and physical activity[4].

In this context, natural compounds represent an attractive possibility, and the use of nutraceuticals for weight loss is increasing[5]. Natural products encompass molecules with enormous structural and chemical diversity. Many studies have shown the potential of phenolic compounds (PC) in modulating gene expression and metabolic pathways, remodeling the epigenetic profile, and potentially contributing to weight loss[5]. PCs are plant-derived compounds characterized by the presence of at least one phenol ring in their molecular structure, and they are classified into 4 main groups: lignans, phenolic acids, flavonoids, and stilbenes. Silybin (2,3-dihydro-3-(4-hydroxy-3-methoxyphenyl)-2-(hydroxymethyl)-1,4-benzodioxin-6-yl]-2,3-dihydro-3,5,7-trihydroxy-4H-1-benzopyran-4-one) is a flavonolignan representing the main active ingredient of silymarin, a PC mixture extracted from the milk thistle Silybum marianum. Milk thistle has been used for thousands of years as a remedy for a variety of conditions due to its anti-inflammatory and hepatoprotective properties[6–8]. Silybin is a strong antioxidant able to reduce inflammation and mitochondrial dysfunction, and a potent lipid lowering agent in NAFLD[9–11]. Carvacrol (2-methyl-5-(1-methylethyl)-phenol) is a phenolic monoterpenoid found in essential oils of many aromatic plants of the Lamiaceae family[12]. Several in vitro and in vivo studies demonstrated that carvacrol possesses a wide range of bioactivities such antimicrobial, antioxidant, and anticancer activities[13–16]. Rosmarinic acid (α-o-caffeoyl-3,4-dihydroxyphenyllactic acid), the ester of caffeic acid, is a phenolic acid abundant in aromatic plants of the Lamiaceae family, known for its antimicrobial, anti-inflammatory, antioxidant effects[17], and for its anti-diabetic potency[18].

Among the endogenous molecules, thyroid hormones are the main controller of the body metabolism[19]. The main bioactive hormone is the 3,5,3'-triiodo-L-thyronine (T_3) which can be deiodinated to the bioactive derivative 3,5-diiodo-l-thyronine (T_2)[20,21]. Thyroid hormones (THs) stimulate lipolysis from fat stores in white adipose tissue and from dietary fat sources to generate circulating free fatty acids (FAs), which are the major source of lipids for the liver. In the liver, THs play catabolic actions by mobilizing lipids[19].

The present study investigated the metabolic effects of three natural phenolic compounds from plants (carvacrol, rosmarinic acid, and silybin), in comparison with two endogenous hormones (T_2 and T_3 hormones), using the cellular models of hepatic steatosis and mature adipocytes, in the attempt to clarify the distinctive molecular mechanisms underlying their beneficial action on different tissues. The research focused on the peroxisome proliferator-activated receptors (PPARs) as they are key regulators of metabolic homeostasis, thus being attractive therapeutic targets for metabolic disorders. PPARs belong to the nuclear hormone receptor superfamily; they bind FAs and FA-derivatives to regulate lipid and carbohydrate metabolism[22], but they act also in inflammation, cell proliferation, and differentiation. In mammals, three subtypes (PPARα, γ, β/δ) are encoded by different genes, and show tissue-specific expression patterns[23,24]. PPARα is found mainly in tissues with high catabolic rate, such as the liver, where it controls expression of FA transporters and enzymes of FA oxidation[25,26]. PPARγ is the main isoform in white adipose tissue, but is also expressed in the healthy liver; in obese patients, PPARγ over-expression seems to correlate positively with liver steatosis[27]. PPARβ/δ is expressed almost ubiquitously, but its role is less clear. The activation of the different PPAR isoforms is coordinated by both natural and synthetic ligands acting as agonists or antagonists to regulate distinct homeostatic pathways. Molecular docking is a computational technique that predicts the binding affinity of ligands to proteins, which have potential applications in nutraceutical research and drug development. Therefore, the present study compared the bioactive compounds in terms of their binding affinity to PPARγ and PPARa, as well as their effect on modulating the expression of the two PPARs. The findings of the present study provide new insights into the molecular mechanism of their action in the different tissues.

Materials and methods

Chemicals

All chemicals, unless otherwise indicated, were supplied by Sigma- Aldrich Corp. (Milan, Italy).

Cell culture and treatments

FaO cells are a rat hepatoma cell line supplied by European Collection of Authenticated Cell Cultures (ECACC, Sigma–Aldrich Corp.). These cells represent a well-differentiated liver cell line expressing a variety of liver-specific functions[28,29] and showing a very stable phenotype[30]. Cells are cultured at 37°C in a humidified atmosphere of 5% CO2. The medium was the Coon's modified Ham's F12 supplemented with 10% heat-inactivated Foetal Bovine Serum (FBS, Euroclone, Milan, Italy). For the in vitro model of hepatic steatosis, FaO cells were seeded on Petri-dishes, and when they reached 80% confluence, they were treated with a mixture of oleate and palmitate (OP) in a 2:1 molar ratio, at a final concentration of 0.75mM in starvation medium (0.25% BSA without FBS)[9]. After 3h, the medium was removed and fresh medium was added containing the following lipid-lowering agents: SIL (50μM), CVL (10μM), RA (10μM), T3 (1μM), and T2 (1μM), alternatively. The incubation with the lipid-

lowering agents was maintained for 24 h. The chemical structures of these compounds are reported in Fig. 1. At the end, the cells were harvested and kept at -80°C for further experimental measurements.

The mouse fibroblasts 3T3-L1 are a pre-adipocyte cell line supplied by the American Type Culture Collection (ATCC, Manassas, VA, USA). 3T3-L1 cells were cultured in Dulbecco's modified Eagle medium (DMEM) supplemented with 10% FBS and 25 mmol/L glucose. The cells were cultured for 2 days to get 70–80% confluence (day 0), and then adipogenic differentiation was induced by adding the adipogenic mix containing 1.7µM insulin, 1µM dexamethasone (DEX), and 500µM 3-isobuthyl-1-methylxanthine (IBMX) to the complete medium. Incubation was maintained for 2 days. Then, the medium was supplemented with complete medium containing insulin alone (1.7µM) and the medium was replaced every 2 days. Simultaneously with the third insulin addition, the cells were treated with one of the lipid-lowering agents, alternatively: SIL (50µM), CVL (10µM), RA (10µM), T3 (1µM), and T2 (1µM). The treatment was maintained for 10 days. At the end of the treatments, the cells were harvested. Figure 2 illustrates both models of hepatosteatosis and adipogenesis over a time-scale manner.

For each experiment, the treatments were performed in quadruplicates. MTT assay was performed on both FaO and 3T3-L1 cells to exclude any cytotoxicity of the different treatments. No significant changes were observed (data not shown).

Protein quantification

The protein content was determined by the Bradford assay using BSA as a standard[31].

Intracellular lipid quantification

At the end of each treatment, both FaO and 3T3 cells were scraped, centrifuged, and lysed to extract lipids using a chloroform–methanol (2:1) mixture, as previously described[32]. The triglyceride content of the cellular samples was quantified using the 'Triglycerides liquid' kit (Sentinel, Milan, Italy). The absorbance was read at 546nm using a Varian Cary 50 spectrophotometer (Agilent, Milan, Italy). Values were normalized for the protein content. Data are expressed as percent TG content relative to controls.

Lipid peroxidation

Lipid peroxidation was determined spectrophotometrically through the thiobarbituric acid reactive substances (TBARS) assay which is based on the reaction of malondialdehyde (MDA;1,1,3,3-tetramethoxypropane) with thiobarbituric acid (TBA)[33]. Briefly, 1 vol. of cell suspension was incubated for 45 min at 95℃ with 2 vol. of TBA solution (0.375% TBA, 15% trichloroacetic acid, 0.25N HCl). Then, 1 vol. of N-butanol was added, and the organic phase was read using a Varian Cary50 spectrophotometer at 532 nm. Results were expressed as pmol MDA/mL per mg protein.

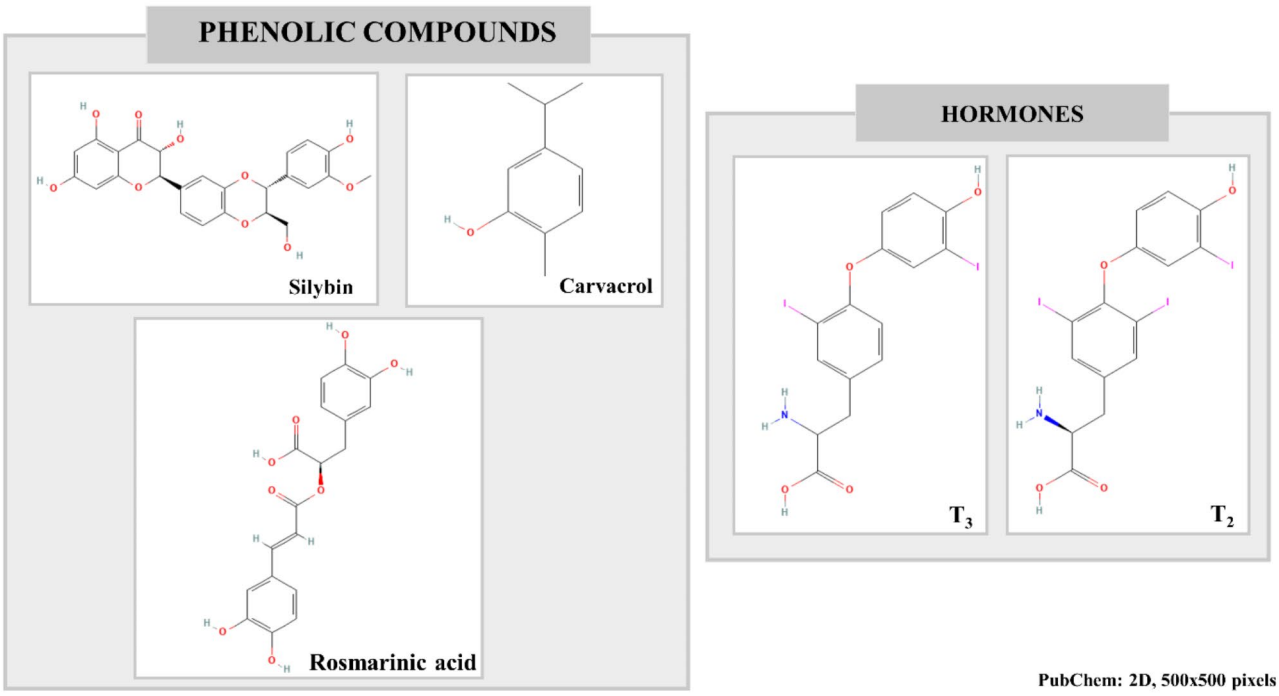

Fig. 1. The 2D chemical structures of the five tested natural products. Three are phenolic compounds: silybin, carvacrol (2-methyl-5-(1-methylethyl)-phenol) and rosmarinic acid (α-o-caffeoyl-3,4-dihydroxyphenyllactic acid). Two are hormones: T3 (3,5,3'-triiodo-L-thyronine) and T2 (3,5-diiodo-l-thyronine) (500 × 500 pixels, https://pubchem.ncbi.nlm.nih.gov/).

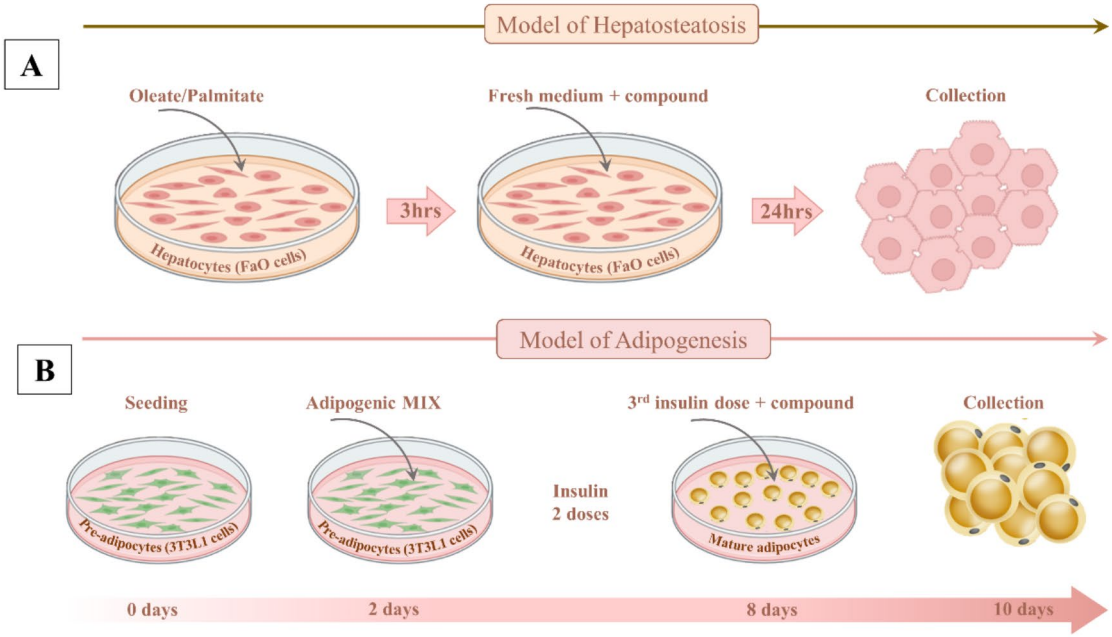

Fig. 2. Schematic representation of the procedure followed to set the in vitro cellular models of hepatosteatosis and adipogenesis used to test the effects of the five natural compounds. For the hepatosteatosis model (**A**), the FaO hepatoma cells were exposed to oleate and palmitate mix for 3h, and then treated with each compound for 24h. For the adipogenesis model (**B**), the 3T3-L1 pre-adipocytes were exposed to the adipogenic mix for 2 days, then to insulin alone; with the third insulin dose each of the five compounds was added and the cells were treated for 2 days.

Gene	primer name	Primer sequence 5'- > 3'
PPARα	Fwd	AAGCCATCTTCACGATGCTG
	Rev	GAGGTCCCTGAACAGTGGCA
PPARγ	Fwd	CGGAGTCCTCCCAGCTGTTCGCC
	Rev	GGCTCATATCTGTCTCCGTCTTC
GAPDH	Fwd	GACCCCTTCATTGACCTCAAC
	Rev	CGCTCCTGGGAAGATGGTGATGGG

Table 1. Primer sequences used for quantitative real-time PCR (qRT-PCR).

RNA extraction and quantitative real-time PCR

Total RNA was isolated from cultured cells by the acid phenol: chloroform procedure using Trizol reagent according to the manufacturers' instructions and then treated with RNase[34]. First strand cDNA was synthesized from total RNA using M-MuLV Reverse Transcriptase (Fermentas, Dasit, Milan, Italy). Quantitative real-time PCR (qPCR) was carried out in quadruplicate using 1 × IQTM SybrGreen SuperMix and Chromo4TM System apparatus (Bio-Rad, Milan, Italy). The relative quantity of target mRNA was calculated using the comparative Cq (represents the cycle number at which the amount of amplified target reaches the fixed threshold) method and was normalized for the expression of glyceraldehyde 3-phosphate dehydrogenase (GAPDH). The expression of the target genes was then calculated as relative quantity of mRNA (fold induction) with respect to controls. Primer pairs were designed ad hoc starting from the coding sequences of Rattus norvegicus and Mus musculus (http:// www.ncbi.nlm.nih.gov/Genbank/GenbankSearch.html) and are listed in Table 1.

In silico docking

Molecular docking is a computational technique used to predict the binding affinity of ligands to receptor proteins. In silico methodology is employed to elucidate the binding mode of compounds at the target site. For docking studies, the structures of bioactive compounds were retrieved from the PubChem website (https://pubchem.ncbi.nlm.nih.gov/) and converted from .mol files to .pdb files using UCSF Chimera software[35].

The structures of the PPARa and of the PPARγ rat transcription factors were obtained with the help of the Swiss-Model server[36] by using as models the human PPARs crystal structures found in Protein Data Bank (pdb-id: 3fur for PPARγ and pdb-id: 3vi8 for PPARa).

We carried out docking calculations using Autodock 4.2 suite of programs (http://autodock.scripps.edu)[37]. The Gasteiger charge calculation method was used, and partial charges were added to the ligand atoms prior to docking. The Lamarckian genetic algorithm (LGA), which is available in Autodock, was employed. Finally, Autodock was used to calculate the binding free energy of each bioactive compound in the PPARa and PPARγ molecular structures. Before docking the bioactive compounds to the PPAR proteins, we utilized the CavityPlus web server[38] to compute the primary docking cavities of the PPAR proteins, which represent larger regions than the specific docking sites.

The binding energy (ΔG in kcal/mol) of each compound with the two PPAR isoforms was evaluated by using Autodock 4.2 software. The higher negative value for ΔG defines the stronger interaction of the ligand with the target site. The Ki (inhibition constant in μM), representing the dissociation constant (Kd) of the protein-inhibitor complex, was also calculated from the binding energy using the formula: $Ki = \exp(\Delta G/RT)$, where R is the universal gas constant (1.985×10^{-3} kcal mol^{-1} K^{-1}) and T is the temperature (298.15 K).

Statistical analysis

Statistical analysis was performed using GraphPad Prism 8 (GraphPad Software Inc., La Jolla, CA, USA, https://graphpad-prism.software.informer.com/8.0/). Differences between groups were compared using one-way ANOVA with post hoc testing. A two-sided p value < 0.05 was considered statistically significant. Continuous variables are presented as mean ± SD.

Results

Metabolic activity of the compounds on steatotic hepatocytes

Upon exposure to oleate/palmitate, FaO hepatocytes increase their TG depots (+ 152% vs Ctrl; $p \leq 0.0001$) thus representing a reliable model of mild hepatic steatosis on which we tested the lipid lowering potential of the five bioactive compounds (Fig. 3). All compounds significantly reduced the TG accumulation of about −149% (CVL), -139% (T2), -125% (T3), −123% (SIL) and −61% (RA) compared to steatotic hepatocytes ($p \leq 0.0001$). Therefore, a similar lipid lowering potential was observed for all the compounds, with rosmarinic acid being the least effective one ($p \leq 0.01$).

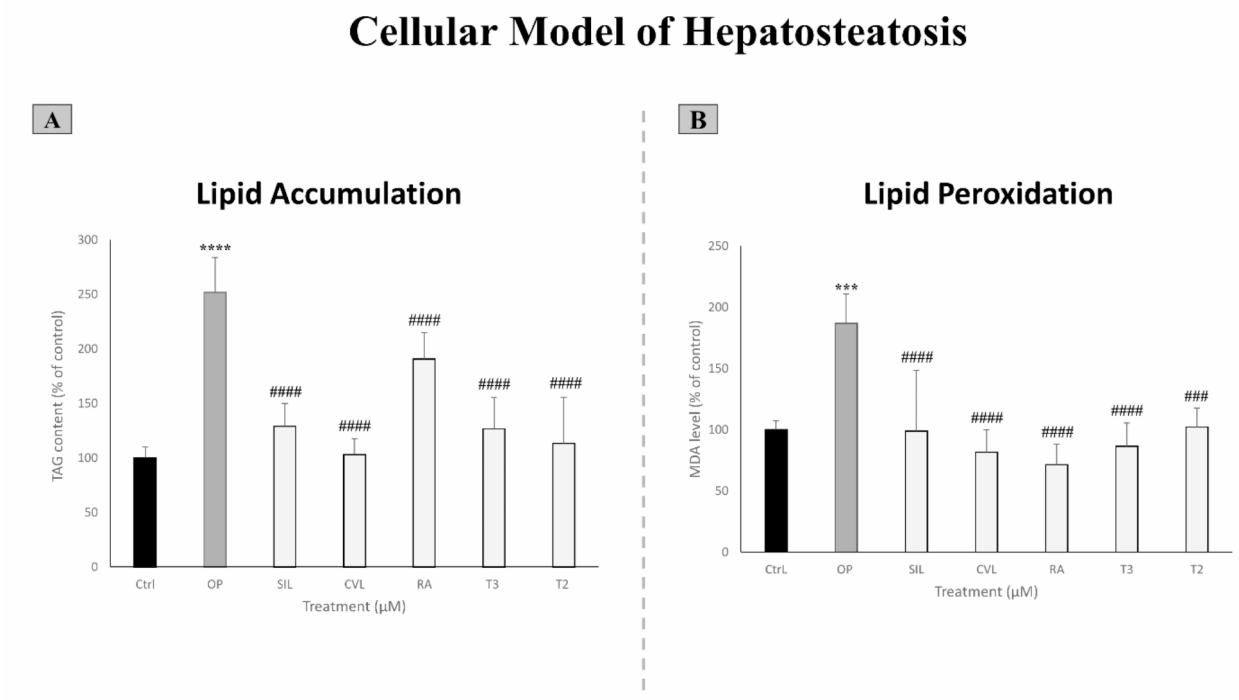

Fig. 3. Metabolic activity of the compounds on steatotic hepatocytes. (**A**) The intracellular TG content quantified by a spectrophotometric assay and expressed as the percentage of TG relative to the control; the TG content was normalized for the protein content determined by the Bradford assay. (**B**) The intracellular level of MDA (pmol MDA/mL × mg of sample protein) quantified by the TBARS assay; data are expressed as percentage values with respect to control and normalized for total proteins. The reported values are mean ± S.D from at least three independent experiments. Statistical significance between groups was assessed by ANOVA, followed by Tukey's test. Significant differences are denoted by symbols: C vs OP $^{***}p \leq 0.001$, $^{****}p \leq 0.0001$, and OP vs different compounds $^{\#\#\#}p \leq 0.001$, $^{\#\#\#\#}p \leq 0.0001$.

The ectopic fat accumulation in hepatocytes typically stimulates ROS over-production due to the stimulation of FA oxidation. In turn, the ROS excess triggers the lipid peroxidation of cellular membranes, a marker for oxidative stress that we quantified in terms of MDA production. In steatotic hepatocytes, we observed an increase in the MDA level compared to control cells (+87%; $p \leq 0.001$) that was reduced after exposure to the single compounds (Fig. 3B). All the bioactive compounds exhibit a similar antioxidant efficacy by reducing the MDA level of -116% (RA), -105% (CVL), -101% (T3), -88% (SIL) ($p \leq 0.0001$), and -85% (T2) ($p \leq 0.001$) respect to steatotic hepatocytes.

Metabolic activity of the compounds on mature adipocytes

The adipogenic differentiation of 3T3 pre-adipocytes to mature adipocytes is accompanied by the accumulation of TGs in cytosolic lipid droplets (+153% with respect to pre-adipocytes; $p \leq 0.0001$). When during adipogenesis the cells were treated with the single compounds, the lipid accumulation was markedly reduced of about -159% (SIL), -147% (CVL), -122% (RA), -123% (T3) and -93% (T2) respect to mature adipocytes ($p \leq 0.0001$) (Fig. 4A). Therefore, we observed a similar lipid-lowering ability for all the compounds with T2 being the least effective one.

Along with adipocyte maturation, we observed a stimulation of ROS generation leading to a significant increase in the MDA level (+136% with respect to pre-adipocytes; $p \leq 0.0001$) (Fig. 4B). A reduction in ROS generation was detected when mature adipocytes were treated with the five compounds: -155% (T3), 134% (CVL), -122% (T2), -113% (SIL), and -102% (RA) respect to mature adipocytes ($p \leq 0.001$). We can highlight that also in adipocytes the five bioactive compounds exhibit a similar antioxidant efficacy, and that the thyroid hormone T3 was the most effective antioxidant agent.

PPAR expression is modulated by the compounds

We investigated the possible effects of the five compounds on the mRNA expression of two PPAR isoforms: PPARγ and PPARα in both hepatocytes and adipocytes (Fig. 5). In steatotic hepatocytes, we observed a significant increase in the PPARγ mRNA expression (2.8-fold induction vs Ctrl, $p \leq 0.0001$), and all the compounds significantly reduced this up-regulation (Fig. 5A). The thyroid hormones T2 and T3 were the most effective in repressing the PPARγ up-regulation (0.6 and 0.5-fold induction vs steatotic hepatocytes, respectively; $p \leq 0.0001$) On the other hand, also the PPARα mRNA expression was up-regulated in steatotic hepatocytes

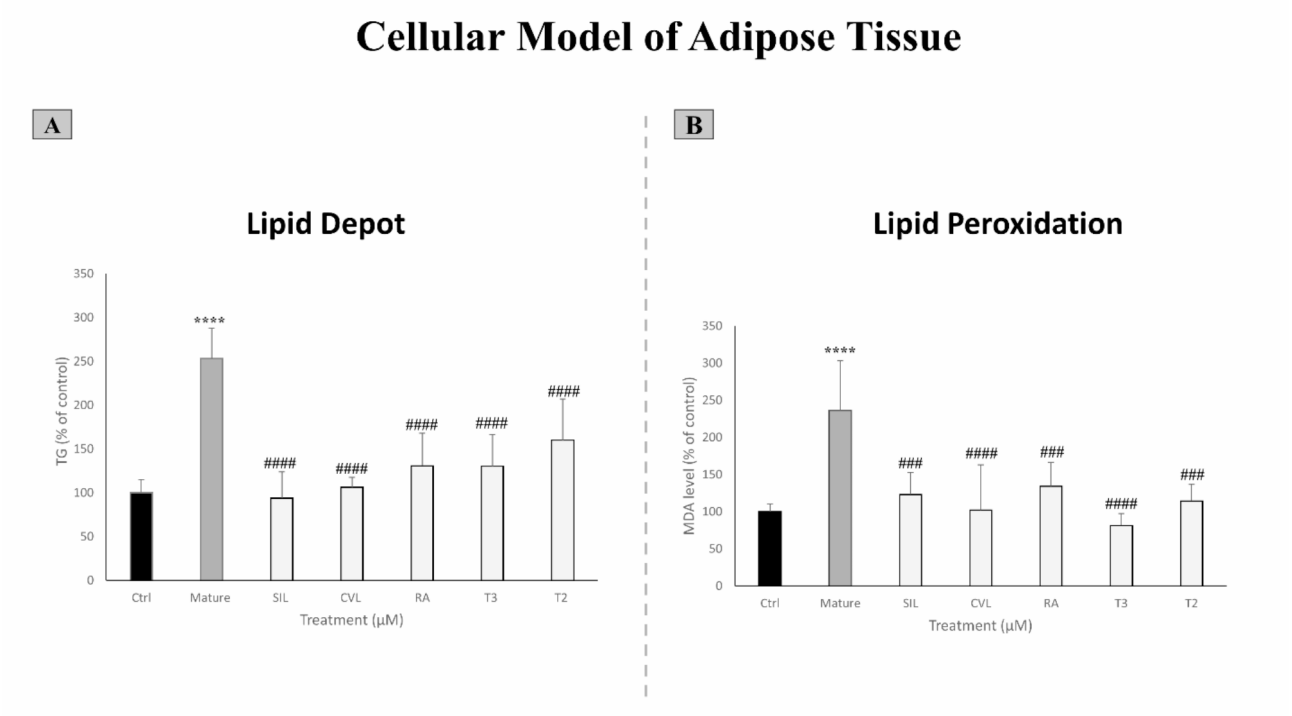

Fig. 4. Metabolic activity of the compounds on adipogenesis. (**A**) The TG accumulation in adipocytes was spectrophotometrically quantified by a spectrophotometric assay during adipocyte maturation and treatment and expressed as the percentage of TG relative to the pre-adipocytes. the TG content was normalized for the protein content determined by the Bradford assay. (**B**) The intracellular level of MDA (pmol MDA/mL × mg of sample protein) quantified by the TBARS assay; data are expressed as percentage values with respect to pre-adipocytes and normalized for total proteins. The reported values are mean ± S.D from at least three independent experiments. Statistical significance between groups was assessed by ANOVA, followed by Tukey's test. Significant differences are denoted by symbols: C vs mature $^{****}p \leq 0.0001$, and mature vs different compounds $^{\#\#\#}p \leq 0.001$, $^{\#\#\#\#}p \leq 0.0001$.

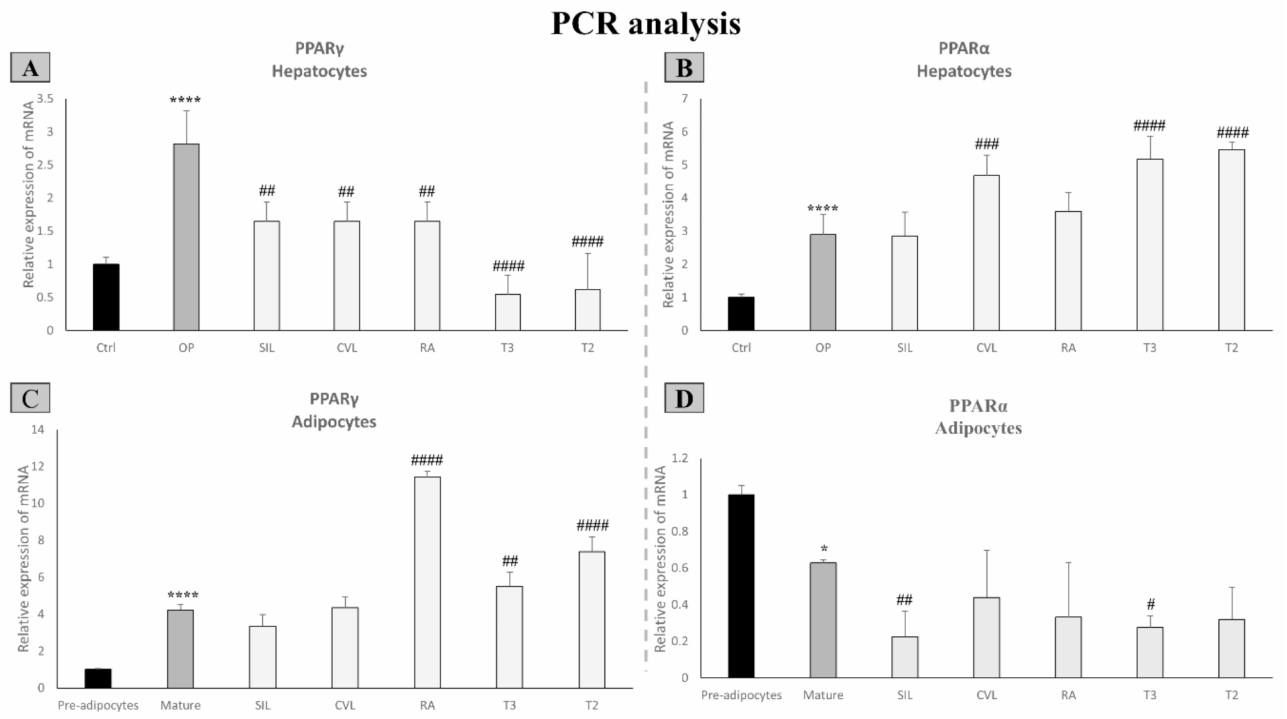

Fig. 5. Molecular effects of the compounds on PPAR expression. Relative mRNA expression of PPARγ and PPARα in both hepatocytes (**A**–**B**) and adipocytes (**C**–**D**) was evaluated by qPCR treated with the five compounds. GAPDH was used as the internal control for quantifying gene expression. Data, expressed with respect to controls, are the mean ± S.D. of at least four experiments in triplicate. Significant differences are denoted by symbols on bars: C vs steatotic/mature $^{*}p \leq 0.05$, $^{****}p \leq 0.0001$, and steatotic/mature vs different compounds $^{\#}p \leq 0.05$, $^{\#\#}p \leq 0.01$, $^{\#\#}p \leq 0.0001$.

(2.89-fold induction vs Ctrl, $p \leq 0.0001$), but in this case a further up-regulation was observed when steatotic hepatocytes were treated with all the compounds except for silybin and rosmarinic acid (Fig. 5B).

In mature adipocytes, the PPARγ mRNA expression was up-regulated by 4.2-fold induction vs pre-adipocytes ($p \leq 0.0001$) to sustain the in vitro adipogenic differentiation (Fig. 5C). Interestingly, the 5 compounds impacted differently on PPARγ transcription. The PPARγ expression was further up-regulated by RA (7.18-fold induction vs mature adipocytes; $p \leq 0.0001$), T2 (3.14-fold induction vs mature adipocytes; $p \leq 0.0001$), and T3 (1.3-fold induction vs mature adipocytes; $p \leq 0.01$), whereas carvacrol and silybin did not modify it. Conversely, mature adipocytes showed a marked decrease in the PPARα mRNA level compared to pre-adipocytes (0.6-fold induction vs pre-adipocytes; $p \leq 0.05$), also in this case the five compounds impacted differently on this PPAR isoform. While carvacrol and rosmarinic acid did not modify significantly the PPARα expression, silybin and T3 further down-regulated the PPARα expression with respect to mature adipocytes (0.41-fold induction and 0.35-fold induction vs mature adipocytes; $p \leq 0.01$ and $p \leq 0.05$, respectively) (Fig. 5D).

Docking results

The binding energy (ΔG) and the inhibition constant (Ki) of each compound with the two PPAR isoforms was evaluated by using Autodock 4.2 software, as described in Materials and Methods. A higher negative value for ΔG defines a stronger interaction of the ligand with the target site. PPARs function as sensors for a variety of molecules that act as agonists or antagonists. As positive controls, we tested two selective agonists of each PPAR. Rosiglitazone and Pioglitazone are standard agonists of PPARγ, belonging to the thiazolidinedione type[39]. Bezafibrate and Clofibrate are PPARα agonists belonging to the fibrate group. Of note, bezafibrate operates as a pan-agonist for all three PPAR isoforms. The docking scores of the five ligands with both PPARγ and PPARα proteins, alongside those of the standard agonists, were listed in Table 2. For all the 5 compounds, we observed the highest docking score with either PPARγ or PPARα within the same cavity bound by the selective agonists, despite some slight differences in the binding sites (Figs. 6, 7).

Regarding PPARγ, the binding domain for the standard agonists Pioglitazone and Rosiglitazone have the following residues in common: ILE309; PHE310; CYS313; ARG316; TYR355; LEU358; LEU361; ILE369; PHE388; PHE391 (Table 2). A ΔG of − 9.05 and -8.17 kcal/mol were calculated for Pioglitazone and Rosiglitazone, respectively, thus indicating that they effectively dock at the PPARγ binding site. Also, the five compounds can be recognized as active agonists based on the negative energy of their docking scores. The docking scores reveal that silybin and T2 have the highest affinity for PPARγ (with Ki values of 0.19 and 0.22 μM, respectively), similar to that predicted for the standard agonist Pioglitazone (Ki 0.23 μM). It is noteworthy that the binding sites of

Protein/receptor	Ligand	Close contacts	Binding energy [kcal/mol]	Ki predicted [mM]
PPARγ	Silybin	PHE310; CYS313; **GLN314**; **ARG316**; SER317; HIS351; TYR355; LEU358; LEU361; **ILE369**; **SER370**; **GLU371**; PHE391; MET392; HIS477; LEU481	-9.19	0.19
	T2	**ASP288**; GLY312; CYS313; ARG316; TYR355; LEU358; VAL367; ILE369; **SER370**; MET376; PHE391; MET392	-9.09	0.22
	T3	**ASP288**; GLY312; CYS313; TYR355; LEU358; VAL367; ILE369; **SER370**; MET376; LEU381; PHE391; MET392	-7.33	4.25
	Carvacrol	PHE310; CYS313; **GLN314**; TYR355; PHE388; PHE391; HIS477	-5.94	46.7
	Rosmarinic acid	PRO255; **LEU256**; ASP288; LYS289; PHE315; **ARG316**; GLU319; **GLU323**; ILE369; **SER370**; GLU371	-5.33	124.7
	Pioglitazone	ALA306; ILE309; PHE310; CYS313; ARG316; **TYR355**; LEU358; LEU361; ILE369; **SER370**; LEU381; PHE388; ***PHE391***; HIS477	-9.05	0.23
	Rosiglitazone	ILE309; PHE310; CYS313; **ARG316**; **TYR355**; LEU358; LEU361; **LEU368**; ILE369; PHE388; ***PHE391***	-8.17	1.03
PPARa	Silybin	**ASN219**; **CYS276**; MET279; GLU286; MET320; LEU321; LEU324; MET330; ILE332; ILE354; **MET355**; LYS358	-10.13	0.04
	T2	***PHE218***; **ASN219**; **MET220**; **CYS276**; MET279; **SER280**; THR283; **GLU286**; ILE317; MET320; LEU321; LEU324	-9.05	0.23
	T3	PHE272; CYS275; CYS276; GLN277; MET279; **SER280**; **TYR314**; ILE317; LEU321; MET330; ILE332; **ALA333**; MET355; **HIS440**; **TYR464**	-8.05	1.25
	Carvacrol	TYR214; **ASN219**; **MET220** ASN221; THR283; **GLU286**; MET320; SER323; LEU324	-6.27	25.6
	Rosmarinic acid	PHE218; **ASN219**; **MET220**; CYS276; **MET279**; **SER280**; **THR283**; **GLU286**; ILE317; MET320; LEU321	-6.85	9.50
	Bezafibrate	CYS276; GLN277; MET279; SER280; **THR283**; **TYR314**; ILE317; MET320; LEU321; **HIS440**; VAL444; **TYR464**	-9.20	0.18
	Clofibrate	CYS276; GLN277; **SER280**; **TYR314**; PHE318; LEU321; ILE354; LYS358; **HIS440**; LEU456; LEU460; **TYR464**	-7.07	6.53

Table 2. Amino acids in close contact, binding affinities and inhibition constant (T = 298.15 K) of the five bioactive compounds and the standard agonists with respect to PPARγ (first part of the Table) and PPARa (second part of the Table). Amino acids that are in close contact and form an H-bond with the corresponding ligand molecule are highlighted in "black bold," while those that have a pi interaction with the corresponding ligand molecule are highlighted in “bolditalic”.

silybin and T2 are slightly different from that of Pioglitazone, sharing 8 and 6 identical amino acids, respectively, with the binding site of Pioglitazone.

Regarding PPARα, the binding domain for the standard agonists Bezafibrate and Clofibrate shares the following amino acid sequence: CYS276, GLN277, SER280, TYR314, LEU321, HIS440, LEU456, and TYR464 (Table 2). A ΔG of -9.20 and -7.07 kcal/mol were calculated for Bezafibrate and Clofibrate, respectively thus indicating that they effectively dock at the PPARα binding site. However, for Clofibrate our calculations indicate a predicted Ki higher than that of Bezafibrate, that suggest a higher affinity of Clofibrate for PPARα. Interestingly, the docking score suggests that silybin exhibits an affinity for PPARα (Ki 0.04 μM) higher than that of the standard agonist Bezafibrate (Ki 0.18 μM), even if there is a slight difference in the residues of the binding site, with silybin sharing only 4 amino acids with Bezafibrate (CYS276, MET279, MET320, LEU321) and Clofibrate (CYS276, LEU321, ILE354, LYS358) binding sites.

Discussion

Due to the escalating epidemic of overweight and obesity, the identification of nutraceuticals with better therapeutic activity and minimal side-effects is of increasing interest for human health. It is of primary importance not only to identify new lipid-lowering candidates, but also to shed the light on the molecular pathways sustaining their beneficial effects. In the present study, we compared the lipid-lowering and antioxidant effect of a pool of natural bioactive compounds, three phenolic compounds and two hormones as physiological comparison, using two different cellular models of fatty liver and adipose tissue. The main findings of this study indicate that, nevertheless a similar metabolic efficacy as lipid-lowering and antioxidant agents, the natural compounds impacted differently on the expression of the two main PPAR isoforms and bind them with different affinity, thus suggesting that different mechanisms might sustain the biological activity of these natural compounds.

Regarding the metabolic effects, our results clearly indicate that all the analyzed compounds are effective lipid lowering and antioxidant agents in steatotic hepatocytes, except the rosmarinic acid which showed poor efficacy against hepatosteatosis. Also in mature adipocytes, all the compounds were able to reduce the fat accumulation and the oxidative stress, and in these cells T_2 was the least effective compound. Of note, regulating the maturation of adipocytes by influencing the lipid metabolism may be of interest for obesity and metabolic disorders, as well as the anti-steatotic effects for fatty liver.

To shed the light on the mechanisms sustaining the action of the five compounds, we focused on the PPARs, as these nuclear receptors act as lipid sensors to connect the nutritional inputs with the reprogram of lipid and glucose homeostasis[40]. Three are the PPAR isoforms that show different tissue distributions and physiological role, and PPARγ and PPARα are the main isoforms in liver and adipose tissue, respectively. Agonists /antagonists

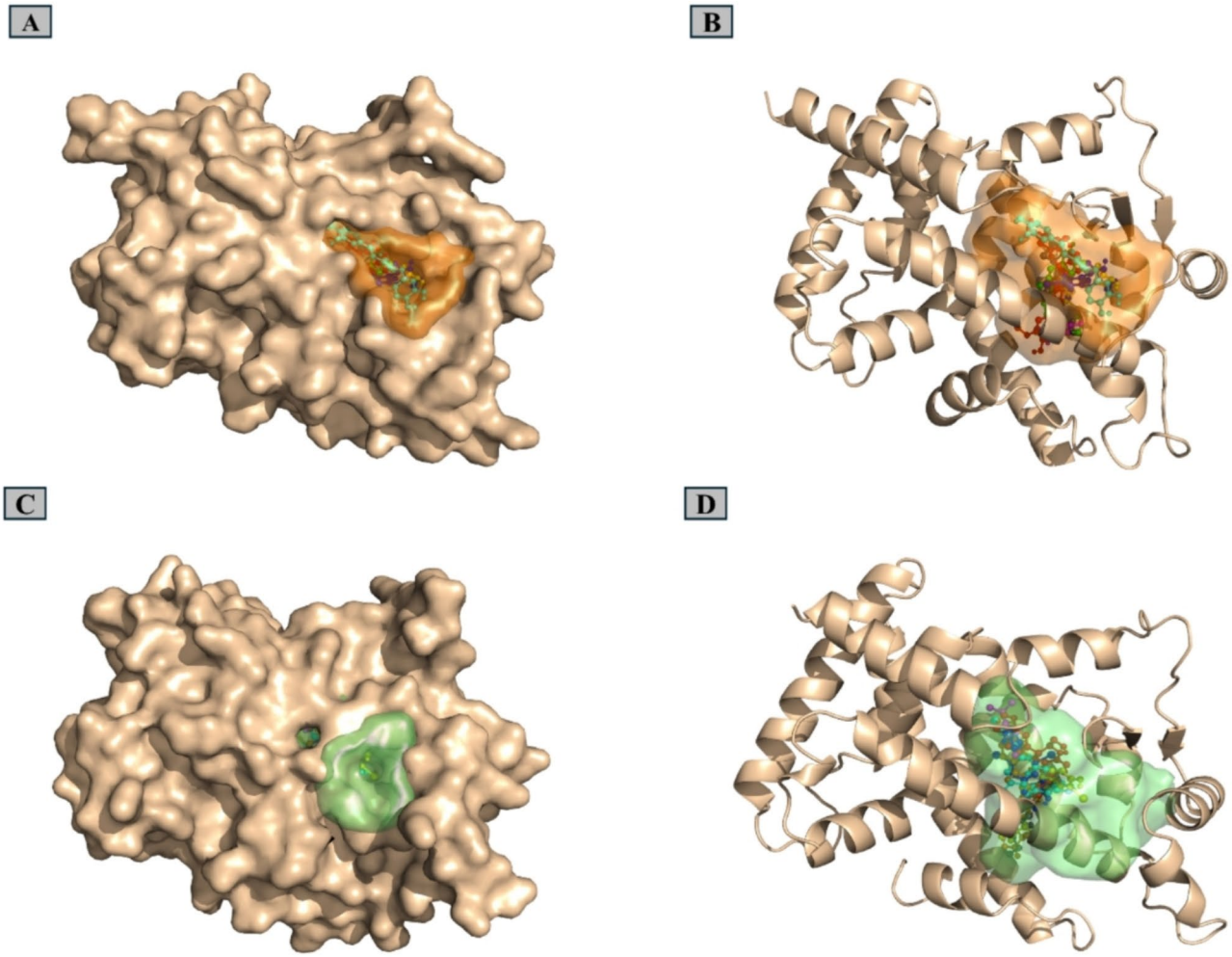

Fig. 6. Molecular docking analyses. (**A**) PPARγ is shown in surface representation in wheat color and binding cavity in orange. (**B**) PPARγ in cartoon and binding cavity in orange. Inside the cavity, in both panels, the five bioactive compounds and the two standard agonists in ball-and-sticks. Silybin red, Carvacrol magenta, Rosmarinic acid cyan, T2 blue, T3 yellow, Pioglitazone green, and Rosiglitazone gray. (**C**) PPARα is shown in surface representation in wheat color and binding cavity in green. (**D**) PPARα in cartoon and binding cavity in orange. Inside the cavity, in both panels, the five bioactive compounds and the two standard agonists in ball-and-sticks. Silybin red, Carvacrol magenta, Rosmarinic acid cyan, T2 blue, T3 yellow, Bezafibrate orange, and Clofibrate gray.

of PPARs are attractive therapeutic approaches in both obesity and NAFLD conditions. PPARα agonists (i.e. fibrates) normalize dyslipidaemia, lipid metabolism, and energy homeostasis, whereas PPARγ agonists (e.g., thiazolidinediones) improve insulin resistance and diabetes[39,41].

When we quantified the mRNA expression of PPARγ and PPARα we could appreciate some interesting differences depending on the compounds and the cell type. In steatotic hepatocytes, PPARγ expression was markedly up-regulated, and all the compounds significantly counteracted this up-regulation, mostly the thyroid hormones. Also, the mRNA expression of PPARα was up-regulated in steatotic hepatocytes, but in this case only the thyroid hormones and carvacrol further increased the mRNA expression while silybin and rosmarinic acid had no effects. Different patterns were identified in mature adipocytes. During adipogenesis, as expected, the mRNA expression of PPARγ was up-regulated, and the thyroid hormones and rosmarinic acid further up-regulated it. By contrast, the mRNA level of PPARα was down-regulated during adipocyte maturation, and all the compounds are very weak modulators of the PPARα transcription. Silybin and T3 further reduced it, while T2, carvacrol, and rosmarinic acid did not affect it.

It is well known that PPARγ is the predominant isoform in adipose tissue, and in the liver of both humans and animal models, increased expression of PPARγ associates with hepatic steatosis. Pioglitazone and rosiglitazone are synthetic agonists of PPARγ which find application as antidiabetic agents to induce insulin sensitization and improve glycemic control in T2DM patients[42–44]. Conversely, PPARα is the main isoform in the liver[45], where it controls genes encoding for FA uptake and β-oxidation. Bezafibrate and clofibrate are synthetic agonists of PPARα which are employed for the treatment of dyslipidemia and obesity (Staels & Fruchart, 2005; Rakhshandehroo et

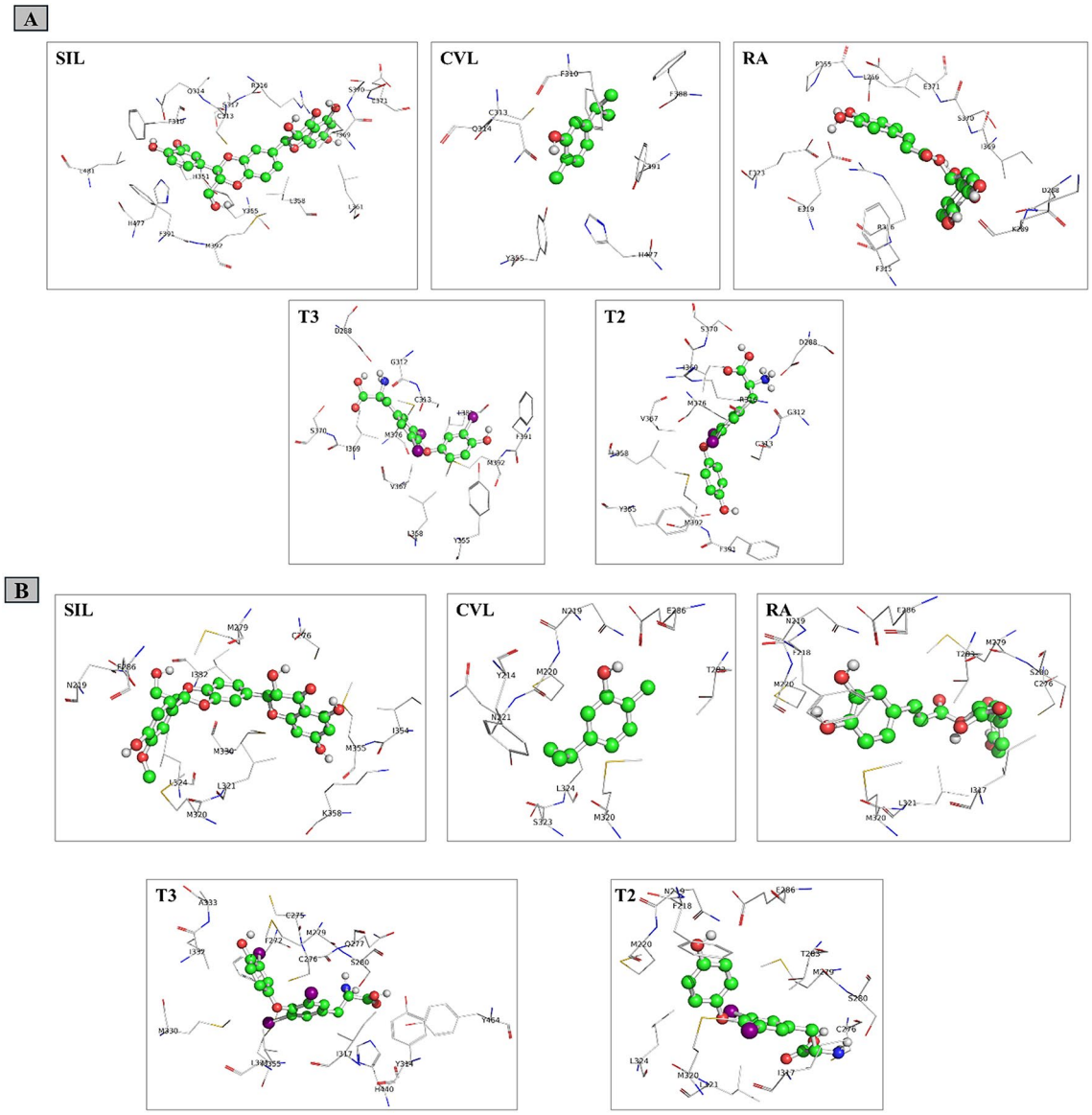

Fig. 7. Structural presentation of the binding sites. (**A**) The binding sites on PPARγ and (**B**) PPARα of the five natural compounds. (**C**) The binding sites of the standard agonists: Pioglitazone and Rosiglitazone (PPARγ), and Bezafibrate and Clofibrate (PPARα).

al., 2010, Corrales et al., 2018). To this regard, our efforts focused on testing the possible binding and affinity of the five compounds with these two PPAR isoforms.

PPARγ protein consists of five domains[48], where the E region is the largest domain representing the ligand-binding domain (LBD), and the C region is the DNA-binding domain (DBD)[49]. FAs are the endogenous agonists of PPARγ but they are weak agonists compared to the synthetic thiazolidinediones (Wang et al. 2014). PPARa protein consists of a N-terminal activating function-1 (AF-1) domain, a central DBD, and a C-terminal LBD. Natural ligands of PPARa include FAs and FA derivatives, as well as molecules with structural resemblance to FAs.

Our molecular docking analysis identified silybin as the phenolic compound with the strongest affinity for both PPARγ and PPARα, when compared with both the standard PPARγ agonist pioglitazone and the standard PPARα agonist bezafibrate. Also, the thyroid hormones, T2 in particular, are effective ligands for both PPARγ and PPARα. Therefore, we can assume that the strong interaction with the two PPAR isoforms may be, at least in part, the main event sustaining the highest metabolic functionality of both silybin and T2. Moreover, our findings are in line with previous reports showing that silybin binds and activates efficiently PPARα[50,51]. Moreover, many studies addressed the effects of natural dietary flavonoids such as quercetin and resveratrol on modulating transcription of PPARγ through agonist binding mode. Quercetin could decrease the level of cholesterol in macrophages via increased PPARγ expression[52], whereas resveratrol has shown to elicit PPARγ stability in 3T3-L1 adipocytes and decrease mRNA and protein levels of PPARγ[53].

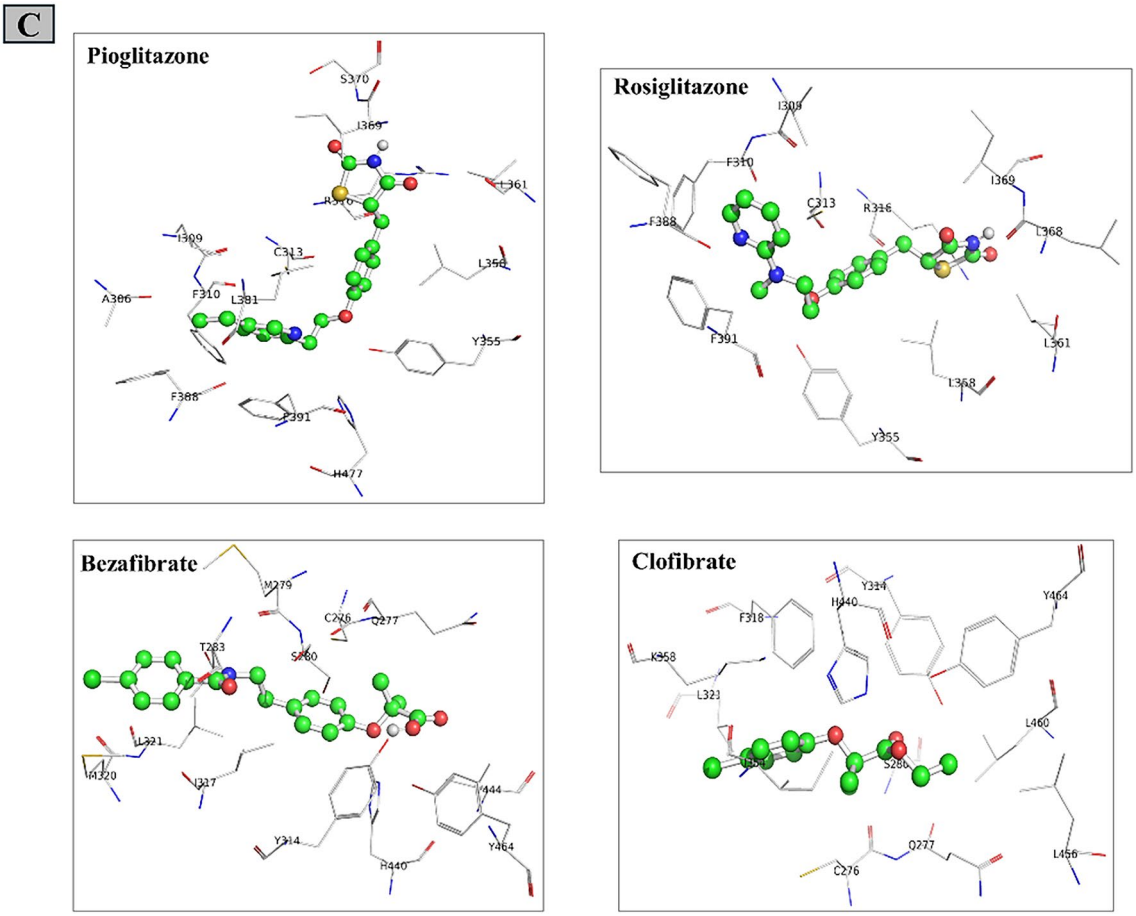

Figure 7. (continued)

It is interesting to note that the compounds under analysis act in a double key on PPARγ and PPARα: they are both modulators of their mRNA expression and agonists by binding them similarly with the standard agonists. Of note, also thiazolidinediones bind and activate PPARγ, and at the same time decrease the PPARγ protein levels.

In conclusion, natural products have proven historically to be a promising pool of structures for drug discovery. A big effort has recently been undertaken to explore the PPARα– and PPARγ-activating potential of a wide range of natural products originating from traditionally used medicinal plants or dietary sources. Many natural PPARγ ligands have been identified showing different binding modes to the receptor in comparison to the full thiazolidinedione agonists, and on some occasions, they were able to activate also PPARα (e.g. genistein). Therefore, our insights demonstrating that silybin and T2 are strong agonists of PPARα, showing an affinity similar to that of the synthetic agonists, and also of PPARγ can suggest their future applications due to the possibility to modulate PPARs activation by dietary interventions or food supplements. In fact, the severe adverse effects of thiazolidinediones led to their restricted clinical applications.

Data availability

"Data is provided within the manuscript, but the data may be provided upon request". Contact the corresponding author: Laura Vergani (laura.vergani@unige.it).

Received: 7 July 2024; Accepted: 30 October 2024
Published online: 15 November 2024

References

1. Karra, P. et al. Metabolic dysfunction and obesity-related cancer: Beyond obesity and metabolic syndrome. *Obesity* **30**, 1323–1334 (2022).
2. Polyzos, S. A., Kountouras, J. & Mantzoros, C. S. Obesity and nonalcoholic fatty liver disease: From pathophysiology to therapeutics. *Metabolism* **92**, 82–97 (2019).
3. Pei, K. et al. An overview of lipid metabolism and nonalcoholic fatty liver disease. *Biomed Res. Int.* **2020**, 1–12 (2020).
4. Salvoza, N., Giraudi, P. J., Tiribelli, C. & Rosso, N. Natural compounds for counteracting nonalcoholic fatty liver disease (NAFLD): Advantages and limitations of the suggested candidates. *Int. J. Mol. Sci.* **23**, 2764 (2022).

5. Vrânceanu, M. et al. Plant-derived nutraceuticals involved in body weight control by modulating gene expression. *Plants* **12**, 2273 (2023).
6. Flora, K., Hahn, M., Rosen, H. & Benner, K. Milk thistle (Silybum marianum) for the therapy of liver disease. *Am. J. Gastroenterol.* **93**, 139–143 (1998).
7. Skottová, N. & Krecman, V. Silymarin as a potential hypocholesterolaemic drug. *Physiol. Res.* **47**, 1–7 (1998).
8. Abenavoli, L., Capasso, R., Milic, N. & Capasso, F. Milk thistle in liver diseases: past, present, future. *Phytother. Res.* **24**, 1423–1432 (2010).
9. Vecchione, G. *et al.* The nutraceutic silybin counteracts excess lipid accumulation and ongoing oxidative stress in an in vitro model of non-alcoholic fatty liver disease progression. *Front. Nutr.* **4**, (2017).
10. Vecchione, G. et al. Silybin counteracts lipid excess and oxidative stress in cultured steatotic hepatic cells. *World J. Gastroenterol.* **22**, 6016 (2016).
11. Grasselli, E. et al. Excess fructose and fatty acids trigger a model of non-alcoholic fatty liver disease progression in vitro: Protective effect of the flavonoid silybin. *Int. J. Mol. Med.* **44**, 705–712 (2019).
12. Diab, F. et al. The potential of lamiaceae herbs for mitigation of overweight, obesity, and fatty liver: studies and perspectives. *Molecules* **27**, 5043 (2022).
13. Khalil, M. *et al.* Antisteatotic and antioxidant activities of *Thymbra spicata* L. extracts in hepatic and endothelial cells as in vitro models of non-alcoholic fatty liver disease. *J. Ethnopharmacol.* **239**, 111919 (2019).
14. Khalil, M. et al. Beneficial effects of carvacrol on in vitro models of metabolically-associated liver steatosis and endothelial dysfunction: A role for fatty acids in interfering with carvacrol binding to serum albumin. *Curr. Med. Chem.* **29**, 5113–5129 (2022).
15. Aristatile, B., Al-Numair, K. S., Veeramani, C. & Pugalendi, K. V. Effect of carvacrol on hepatic marker enzymes and antioxidant status in d-galactosamine-induced hepatotoxicity in rats. *Fundam. Clin. Pharmacol.* **23**, 757–765 (2009).
16. Kim, E., Choi, Y., Jang, J. & Park, T. Carvacrol protects against Hepatic steatosis in mice fed a high-fat diet by enhancing SIRT1-AMPK signaling. *Evidence-Based Complement. Altern. Med.* **2013**, 1–10 (2013).
17. Nadeem, M. et al. Therapeutic potential of rosmarinic acid: A comprehensive review. *Appl. Sci.* **9**, 3139 (2019).
18. Jayanthy, G. & Subramanian, S. RA abrogates hepatic gluconeogenesis and insulin resistance by enhancing IRS-1 and AMPK signalling in experimental type 2 diabetes. *RSC Adv.* **5**, 44053–44067 (2015).
19. Sinha, R. A., Singh, B. K. & Yen, P. M. Direct effects of thyroid hormones on hepatic lipid metabolism. *Nat. Rev. Endocrinol.* **14**, 259–269 (2018).
20. de Lange, P. et al. Nonthyrotoxic prevention of diet-induced insulin resistance by 3,5-diiodo-L-thyronine in rats. *Diabetes* **60**, 2730–2739 (2011).
21. Vergani, L. Lipid lowering effects of iodothyronines: In vivo and in vitro studies on rat liver. *World J. Hepatol.* **6**, 169 (2014).
22. Kersten, S., Desvergne, B. & Wahli, W. Roles of PPARs in health and disease. *Nature* **405**, 421–424 (2000).
23. Braissant, O., Foufelle, F., Scotto, C., Dauça, M. & Wahli, W. Differential expression of peroxisome proliferator-activated receptors (PPARs): tissue distribution of PPAR-alpha, -beta, and -gamma in the adult rat. *Endocrinology* **137**, 354–366 (1996).
24. Grygiel-Górniak, B. Peroxisome proliferator-activated receptors and their ligands: nutritional and clinical implications: A review. *Nutr. J.* **13**, 17 (2014).
25. Chakravarthy, M. V. et al. "New" hepatic fat activates PPARα to maintain glucose, lipid, and cholesterol homeostasis. *Cell Metab.* **1**, 309–322 (2005).
26. Mandard S, Müller M, K. S. Peroxisome proliferator-activated receptor a target genes. *Cell. Mol. Life Sci.* **61**, 393–416 (2004).
27. Pettinelli, P. & Videla, L. A. Up-regulation of PPAR-γ mRNA expression in the liver of obese patients: an additional reinforcing lipogenic mechanism to SREBP-1c induction. *J. Clin. Endocrinol. Metab.* **96**, 1424–1430 (2011).
28. Clayton, D. F., Weiss, M. & Darnell, J. E. Liver-specific RNA Metabolism in hepatoma cells: Variations in transcription rates and mRNA levels. *Mol. Cell. Biol.* **5**, 2633–2641 (1985).
29. Lauris, V., Crettaz, M. & Kahn, C. R. Coordinate roles of insulin and glucose on the growth of hepatoma cells in culture. *Endocrinology* **118**, 2519–2524 (1986).
30. Deschatrette, J. & Weiss, M. C. Characterization of differentiated and dedifferentiated clones from a rat hepatoma. *Biochimie* **56**, 1603–1611 (1975).
31. Bradford, M. M. A rapid and sensitive method for the quantitation of microgram quantities of protein utilizing the principle of protein-dye binding. *Anal. Biochem.* **72**, 248–254 (1976).
32. Vergani. PAT protein mRNA expression in primary rat hepatocytes: effects of exposure to fatty acids. *Int. J. Mol. Med.* **25**, 505–512 (2010).
33. Iguchi, H., Kojo, S. & Ikeda, M. Lipid peroxidation and disintegration of the cell membrane structure in cultures of rat lung fibroblasts treated with asbestos. *J. Appl. Toxicol.* **13**, 269–275 (1993).
34. Chomczynski, P. & Sacchi, N. Single-step method of RNA isolation by acid guanidinium thiocyanate-phenol-chloroform extraction. *Anal. Biochem.* **162**, 156–159 (1987).
35. Pettersen, E. F. et al. UCSF chimera: A visualization system for exploratory research and analysis. *J. Comput. Chem.* **25**, 1605–1612 (2004).
36. Waterhouse, A. et al. SWISS-MODEL: Homology modelling of protein structures and complexes. *Nucleic Acids Res.* **46**, W296–W303 (2018).
37. Morris, G. M. et al. AutoDock4 and AutoDockTools4: Automated docking with selective receptor flexibility. *J. Comput. Chem.* **30**, 2785–2791 (2009).
38. Xu, Y. et al. CavityPlus: A web server for protein cavity detection with pharmacophore modelling, allosteric site identification and covalent ligand binding ability prediction. *Nucleic Acids Res.* **46**, W374–W379 (2018).
39. Wang, L. et al. Natural product agonists of peroxisome proliferator-activated receptor gamma (PPARγ): A review. *Biochem. Pharmacol.* **92**, 73–89 (2014).
40. Evans, R. M., Barish, G. D. & Wang, Y.-X. PPARs and the complex journey to obesity. *Nat. Med.* **10**, 355–361 (2004).
41. Corrales, P., Vidal-Puig, A. & Medina-Gómez, G. PPARs and metabolic disorders associated with challenged adipose tissue plasticity. *Int. J. Mol. Sci.* **19**, 2124 (2018).
42. Bedoucha, M., Atzpodien, E. & Boelsterli, U. A. Diabetic KKAy mice exhibit increased hepatic PPARγ1 gene expression and develop hepatic steatosis upon chronic treatment with antidiabetic thiazolidinediones. *J. Hepatol.* **35**, 17–23 (2001).
43. Gurnell, M., Savage, D. B., Chatterjee, V. K. K. & O'Rahilly, S. The metabolic syndrome: Peroxisome proliferator-activated receptor γ and its therapeutic modulation. *J. Clin. Endocrinol. Metab.* **88**, 2412–2421 (2003).
44. Sanyal, A. J. et al. Pioglitazone, Vitamin E, or Placebo for nonalcoholic steatohepatitis. *N. Engl. J. Med.* **362**, 1675–1685 (2010).
45. Pawlak, M., Lefebvre, P. & Staels, B. Molecular mechanism of PPARα action and its impact on lipid metabolism, inflammation and fibrosis in non-alcoholic fatty liver disease. *J. Hepatol.* **62**, 720–733 (2015).
46. Staels, B. & Fruchart, J.-C. Therapeutic roles of peroxisome proliferator-activated receptor agonists. *Diabetes* **54**, 2460–2470 (2005).
47. Rakhshandehroo, M., Knoch, B., Müller, M. & Kersten, S. Peroxisome proliferator-activated receptor alpha target genes. *PPAR Res.* **2010**, 1–20 (2010).
48. Chandra, V. et al. Structure of the intact PPAR-γ–RXR-α nuclear receptor complex on DNA. *Nature* **456**, 350–356 (2008).
49. Kroker, A. J. & Bruning, J. B. Review of the structural and dynamic mechanisms of PPAR γ partial agonism. *PPAR Res.* **2015**, 1–15 (2015).

50. Wang, H. et al. Mechanism-based inhibitory and peroxisome proliferator-activated receptor α-dependent modulating effects of silybin on principal hepatic drug-metabolizing enzymes. *Drug Metab. Dispos.* **43**, 444–454 (2015).
51. Liu, X. et al. Silibinin-induced autophagy mediated by PPARα-sirt1-AMPK pathway participated in the regulation of type I collagen-enhanced migration in murine 3T3-L1 preadipocytes. *Mol. Cell. Biochem.* **450**, 1–23 (2019).
52. Lee, S.-M., Moon, J., Cho, Y., Chung, J. H. & Shin, M.-J. Quercetin up-regulates expressions of peroxisome proliferator-activated receptor γ, liver X receptor α, and ATP binding cassette transporter A1 genes and increases cholesterol efflux in human macrophage cell line. *Nutr. Res.* **33**, 136–143 (2013).
53. Floyd, Z. E., Wang, Z. Q., Kilroy, G. & Cefalu, W. T. Modulation of peroxisome proliferator–activated receptor γ stability and transcriptional activity in adipocytes by resveratrol. *Metabolism* **57**, S32–S38 (2008).

Acknowledgements

This work was supported by grants from the University of Genova (FRA 2020). Part of this work benefits the PRIMA 2022-B4HT_Prima 2022_00124 "Box for Health by Tradition & Innovation: promoting sustainable mediterranean diet by Healthy Foods Progetto" (CUP D33C22002150007).

Author contributions

All authors contributed to this work significantly. FD carried out spectrophotometric experiments, performed real-time PCR and statistical analysis, and wrote the manuscript. HZ carried out the FaO cell growth and treatments. LZ carried out the adipocyte culture and adipogenesis. FB contributed to real-time PCR. AP participated in the study design and data interpretation. VM conducted the molecular docking analyses and contributed to writing the manuscript. LV conceived, designed and supervised the study, wrote, and reviewed the manuscript.

Declarations

Competing interests

The authors declare no competing interests.

Additional information

Correspondence and requests for materials should be addressed to L.V.

Reprints and permissions information is available at www.nature.com/reprints.

Publisher's note Springer Nature remains neutral with regard to jurisdictional claims in published maps and institutional affiliations.